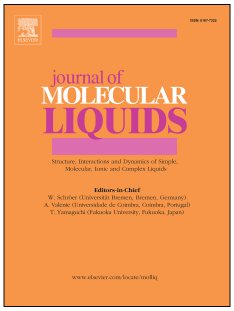

Borohydride-free catalytic reduction of organic pollutants by platinum nanoparticles supported on cellulose fibers

Md Tariqul Islam, Kazi Afroza Sultana, Juan C. Noveron

PII: S0167-7322(19)33863-2

DOI: https://doi.org/10.1016/j.molliq.2019.111988

Reference: MOLLIQ 111988

To appear in: *Journal of Molecular Liquids*

Received Date: 10 July 2019

Revised Date: 7 October 2019

Accepted Date: 20 October 2019

Please cite this article as: M.T. Islam, K.A. Sultana, J.C. Noveron, Borohydride-free catalytic reduction of organic pollutants by platinum nanoparticles supported on cellulose fibers, *Journal of Molecular Liquids* (2019), doi: https://doi.org/10.1016/j.molliq.2019.111988.

Borohydride-free catalytic reduction of organic pollutants by platinum nanoparticles supported on cellulose fibers

Md. Tariqul Islam,[abc*] Kazi Afroza Sultana,[d] Juan C. Noveron [ab*]

[a] Department of Chemistry and Biochemistry, University of Texas at El Paso, 500 West University Avenue, El Paso, TX 79968, USA

[b] NSF Nanosystems Engineering Research Center for Nanotechnology Enabled Water Treatment (NEWT)

[c] Department of Chemistry, University of Texas of the Permian Basin, 4901 E University Blvd, Odessa, TX 79762

[d] Department of Environmental Science and Engineering, University of Texas at El Paso, 500 West University Avenue, El Paso, TX 79968, USA

Keywords: Hydrogen gas, reducing agent, catalytic reduction, platinum nanoparticles, sodium rhodizonate, cellulose fibers.

Abstract

This study presents hydrogen gas-assisted reduction of organic pollutants *viz.* 4-nitrophenol (4-NP) and methyl orange (MO) by platinum nanoparticles (PtNPs) immobilized on cellulose fibers (CF). Because sodium borohydride ($NaBH_4$) causes secondary pollution in water by its decomposition products, hydrogen (H_2) gas was used as a clean, highly active, and alternative reducing agent. As the catalyst, PtNPs of about 2 nm in diameter were synthesized and supported on CF by employing a facile method. The nanocomposites (PtNPs@CF) demonstrated excellent catalytic activity and cyclic stability in the reduction of 4-NP and MO using H_2 gas as the clean, environmentally friendly, highly reactive, and an alternative reducing agent to $NaBH_4$. The catalytic reduction followed the pseudo-first-order reaction kinetic with apparent rate constants of 3.6×10^{-1} min^{-1} and 5.3×10^{-1} min^{-1} for 4-NP and MO, respectively. The

results of this study further indicate that the H_2 gas (reducing agent) and PtNPs@CF nanocomposite (catalyst) can potentially be used for the reduction of a wide variety of other organic and inorganic compounds in water.

1. Introduction

Platinum nanoparticles (PtNPs) possess extraordinary catalytic properties.[1,2] Although bulk or macroscopic platinum is one of the most inert and catalytically inactive materials on earth, platinum in the in the nanoscopic size range (1-100 nm) is extremely catalytically active.[3,4] With the decrease in particle size, the proportion of platinum atoms having the low-coordinated surface sites (edges and corners of the nanocrystal) increases that provide excellent and exotic catalytic activity compared to the atoms in the bulk of the particles, Figure 1 a (inset). These low-coordinated platinum atoms are highly active in carrying out a number of catalytic reactions.[3,4] The size, shape, and composition of the PtNPs further determine the activity and selectivity of the catalytic processes.[5] These parameters also determine electronic, optical, and physical properties of the nanoparticles. In terms of catalysis, some of the widely studied and employed chemical transformations that PtNPs catalyze are reductions,[6,7] oxidations,[8,9] and coupling.[10]

Catalytic reduction has become one of the prominent methods for the degradation or deactivation of organic and inorganic pollutants in water.[11,12,13] For example, the catalytic reduction of has been reported to be an efficient method for the degradation or deactivation of pollutants such as hexavalent chromium, organic dyes, and antibiotics. Especially, catalytic reduction of 4-NP is one of the most widely studied reaction that is performed in academia to evaluate the activity of a newly-developed catalysts such as the noble/transition metal nanoparticles and their nanocomposites.[14,15] In addition of being a model reaction, the reaction is employed in industry as the reduced product *viz.* 4-aminophenol (4-AP) has industrial applications. For instance, 4-AP is used in dyeing textiles, hair, furs, feathers; used as a photographic developer, antioxidants, oil additives; used in pharmaceuticals;[16] an intermediate in the manufacture of sulfur and azo dyes.[17,18] Because the reducing property, it is used as a corrosion inhibitor in paints and as an anticorrosion-lubricating agent in 2-cycle engine fuels.[16] Additionally, 4-AP is used as a wood stain and in imparting a roselike color to timber.[19] For the catalytic reduction of 4-NP and other organic pollutants, excess $NaBH_4$ is used most often as the reducing agent.[20,21,22] However, the major drawback of $NaBH_4$ is that it causes secondary pollution by its excess use and its decomposition by-products such as $B(OH)_3$, $B(OH)_4^-$, BO_2^-, BO_3^{3-}. Moreover, the removal of the excess $NaBH_4$ and its decomposition products becomes even more challenging and cumbersome job. Therefore, there is a need for the development of a cleaner and alternative reducing agent for the reduction organic and inorganic pollutants without causing secondary pollution.

In this regard, neat H_2 gas could be considered as a cleaner an alternative reducing agent for the remediation of environmental pollutants. The utilization of H_2 gas is very common in organic synthesis for the hydrogenation/reduction of organic compounds; however, there are few reports for its utilization towards the reductive degradation of organic pollutants such as 4-NP and MO in water. For example, Lowry Gregory and Martin Reinhard reported the hydrodehalogenation of halogenated organic compounds in water using a palladium catalyst and H_2 gas.[23] However, for the reduction of 4-NP or nitro aromatic compounds, the use of H_2 gas as the reducing agent has not been reported, thus far, to the best of our knowledge.

In this study, H_2 gas-assisted catalytic reduction of 4-NP and MO on PtNPs immobilized on cellulose fibers is reported. PtNPs of about 2 nm in size were synthesized in water by the use of sodium rhodizonate as the reducing-plus-stabilizing agents. Cellulose fibers were used as a solid catalyst support to 1) avoid the energy-intensive separation processes of the PtNPs, 2) prevent the loss of the PtNPs, and 3) prevent the aggregation and/or agglomeration of the PtNPs. The CF, used in this study, was obtained from Kimwipe paper because it demonstrated high binding affinity for PtNPs and good chemical and mechanical stability. Transmission electron microscopy revealed that PtNPs of about 2 nm in size were successfully immobilized to the cellulose fibers. The PtNPs bound CF nanocomposite (PtNPs@CF) was applied as highly active and reusable catalyst for the reduction of 4-NP and MO in water using neat H_2 gas as the clean and environmentally friendly reducing agent alternative to $NaBH_4$.

2. Materials and Methods

2.1. Materials

All chemicals were used as received, unless otherwise mentioned. Sodium rhodizonate dibasic (97%), hydrogen hexachloroplatinate (IV) hydrate (H_2PtCl_6 $3H_2O \geq 99.9\%$), 4-NP, and MO, were purchased from Sigma Aldrich. Kimtech kimwipe paper was purchased from Fisher Scientific, USA. Ultrapure H_2 gas (99.99%) was obtained from Matheson Tri-Gas and Milli-Q water (> 18.20 MI cm resistivity) was obtained from Milli-Q (Advantage A-10) water filter system.

2.2. Characterization Techniques

Hitachi H-7650 transmission electron microscope (TEM) with an accelerating voltage of 80 kV was used to obtain TEM images. Carbon coated copper grid with 200 mesh (Electron Microscopy Science) were used for TEM imaging. The grid was prepared by drop casting method. ImageJ software was used to analyze the average diameter and size distribution of PtNPs from the TEM image. Scanning electron microscopy (SEM) image was obtained by using Hitachi S-3400N Type II scanning electron microscope (SEM) having an accelerating voltage of

15 kV. The X-ray diffraction pattern was obtained Bruker D8 Discover XRD having Cu Kα radiation. The XPS analysis was performed by using Thermo Scientific Escalab 250Xi spectrometer with a six-channel detector. Photoelectrons were generated with a monochromatic Al Ka (1486.68 eV) X-ray source. Agilent Cary 50 Conc UV-Visible spectrophotometer was employed to obtain the UV-visible spectrum. Standard quartz cuvette having path length of 10 mm was used for the UV-visible studies.

2.3. Synthesis of PtNPs and PtNPs@CF

The synthesis of PtNPs was adopted from our previously reported studies.[4] In details, 20 mL of 0.5 mM aqueous solution of chloroplatinic acid was brought to a boil in a 100 mL round-bottomed flask and then 5 mL of 9.7 mM aqueous solution of sodium rhodizonate was added with vigorous stirring (1200 rpm). The reaction mixture was further boiled for 5 min, which was followed by the cooling under the ambient conditions. It could be noted that the synthesis of PtNPs could also be carried out at room temperature by stirring the solution of chloroplatinic acid and sodium rhodizonate for about 20 min of time. For this study, the PtNPs that were synthesized at boiling conditions.

After cooling the reaction, a single sheet of Kimwipe paper (~456 mg) was immersed into the reaction flask whilst shaking by hand for about 5 min. This caused the binding of PtNPs on the Kimwipe paper and the color of the paper changed from white to grey. After rinsing with deionized water, the PtNPs bound Kimwipe paper (PtNPs@CF) was used for catalytic applications. ICP-OES was performed on the supernatant and the rising solution, which confirmed more than 99 % binding ability of the PtNPs on the Kimwipe paper. Thus, the weight percent of the PtNPs on the Kimwipe paper was calculated to be 0.87 %.

2.4. Catalytic reduction of 4-NP and MO on PtNPs@CF

The catalytic reduction of 4-NP and MO was carried out under ambient conditions and at normal pH. Same experimental conditions were adopted for the reduction of 4-NP and MO. The only difference was in their initial concentrations, which were 0.1 mM and .0611 mM for 4-NP and MO, respectively. The experimental procedure for the reduction of 4-NP is mentioned in detail. In 125 mL Erlenmeyer flask, 100 mL of 0.1mM 4-NP solution was taken. A full Kimwipe paper bound with PtNPs was immersed into the 4-NP solution. The flask was sealed with a rubber septum. Afterward, H_2 gas was bubbled into the flask with gentle stirring of the reaction mixture. Hydrogen gas was bubbled by using a balloon connected with a long-stemmed stainless-steel needle. In order to allow continuous bubbling of the H_2 gas a second needle was used to poke the rubber septum, which facilitated the exit of the escaping gas. The reduction of 4-NP was monitored in every 2 minutes period of time by using UV-visible spectrophotometer. About 1 mL aliquots were taken out at a regular interval and the sample was reintroduced into the reaction flask after the UV-visible spectroscopic analysis. The UV-visible spectrophotometer monitored the lowering of the characteristic absorption band of 4-NP at 320 nm. With the gradual lowering of the absorption band at 320 nm a new band originated at 300 nm, which indicated the formation of 4-AP from 4-NP. For MO reduction, the characteristic absorption band that was monitored for its reduction followed by the calculation of percent reduction was 464 nm.

Cyclic stability of the PtNPs@CF was studied by repeating the reduction of MO for 6 cycles. The PtNPs@CF was rinsed with deionized water before the subsequent cycles of use. In every cycle the percent reduction of MO was calculated after 10 min of catalytic reaction.

3. **Characterization of PtNPs and PtNPs@CF**

Various techniques such as Transmission electron microscopy (TEM), Scanning electron microscopy (SEM), X-ray diffraction spectroscopy (XRD), and X-ray photoelectron spectroscopy (XPS) were utilized to thoroughly characterize the PtNPs and the PtNPs@CF. For example, TEM and SEM revealed the morphology of the PtNPs and PtNPs@CF. The binding of the PtNPs to the CF was visualized by the TEM images. High-resolution TEM microscopy image further revealed the atomic resolution image of the PtNPs showing the lattice fringes. The X-ray diffraction pattern demonstrated the crystalline structure of the PtNPs and cellulose fibers in the nanocomposite.[24] The XPS study further provided the elemental composition and the functional groups of the PtNPs@CF.[25]

The morphological information such as the size and shape of the PtNPs were obtained from the TEM images. As shown in Figure 1a, the PtNPs (before binding with CF) could be observed as spherical in shape. The size of the PtNPs were distributed between 0.75 to 4.5 nm with an average of ~2 nm in diameter, Figure 1b. The PtNPs were seen mostly individual although some aggregations were also observed. High-resolution TEM image showed the arrays of Pt atoms in the nanoparticles, Figure 1a (inset). Further, the lattice spacing of 0.23 nm indicated the gap between Pt (111) lattice fringes.[26]

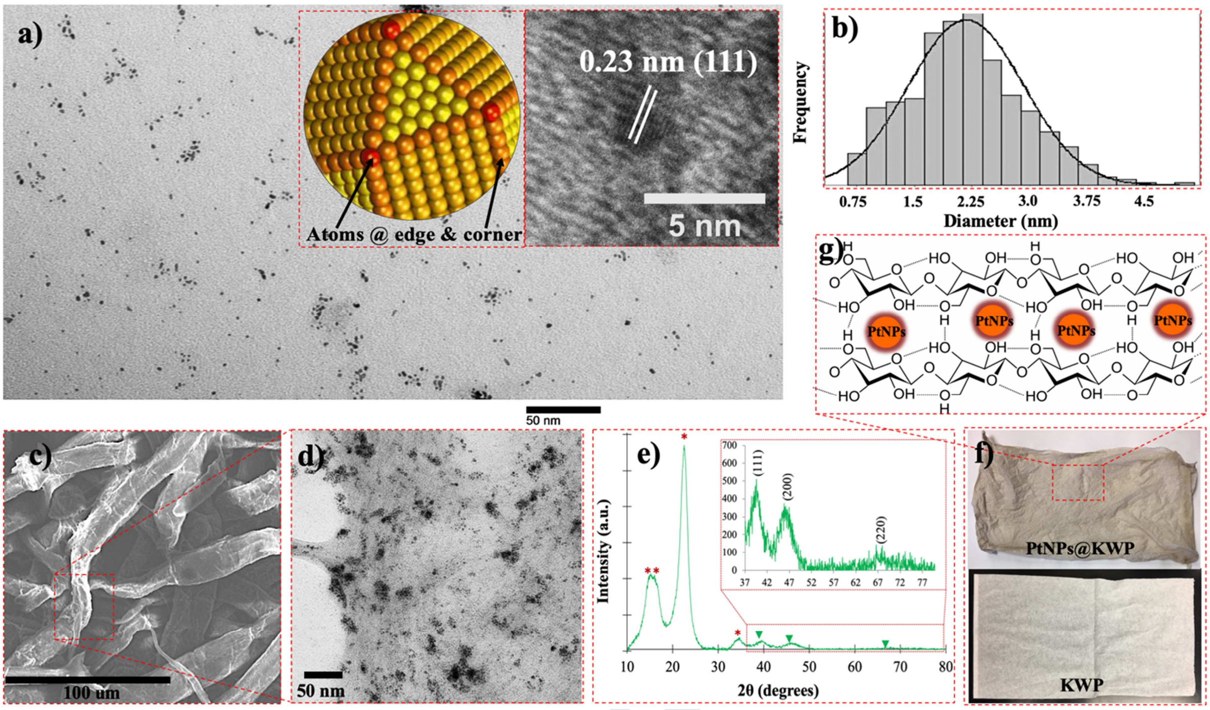

Figure 1. a) Typical and high-resolution TEM images of the as-prepared PtNPs in water, b) size-distribution of the PtNPs, c) SEM image of the PtNPs@CF, d) TEM image of the PtNPs@CF, e) XRD pattern of the PtNPs@CF, f) digital photographic images of the pristine kimwipe paper and PtNPs bound kimwipe paper, and possible binding interaction of the PtNPs with cellulose. Inset (1a): nanocrystal showing relatively more exposed atoms at the corners and edges.

The morphology of the PtNPs@CF was analyzed by the SEM image, Figure 1c. It revealed the fibrous/filamentous morphology of the cellulose fibers having high aspect ratio with a diameter of about 20 μm. Because the PtNPs were too small, they could hardly be seen in the SEM image. Therefore, TEM image was obtained on the PtNPs@CF to visualize the PtNPs, Figure 1d. The TEM image clearly demonstrated that the PtNPs were decorated on the surface of the CF. The PtNPs supported on the CF was found to be somewhat more aggregated compared to the PtNPs in solution.

The XRD pattern of the PtNPs@CF revealed the crystalline property of the cellulose fibers and the PtNPs, Figure 1e. It was found that the CF was highly crystalline. The diffraction peaks located at 2θ = 15.4°, 16.2° and 22.7° corresponds to the Iα, or Iβ allomorphs cellulose.[27,28] Additionally, relatively weak diffraction peaks at 39.8°, 46.4°, and 67.7° corresponds to the metallic crystalline nature of the PtNPs, Figure 1e. Diffraction peaks at 39.8°, 46.4°, and 67.7° are characteristic to the (111), (200), and (220) lattice planes of the completely reduced or metallic (Pt^0) nanoparticles, which further confirms the face-centered cube (fcc) crystalline structure of the PtNPs.[29]

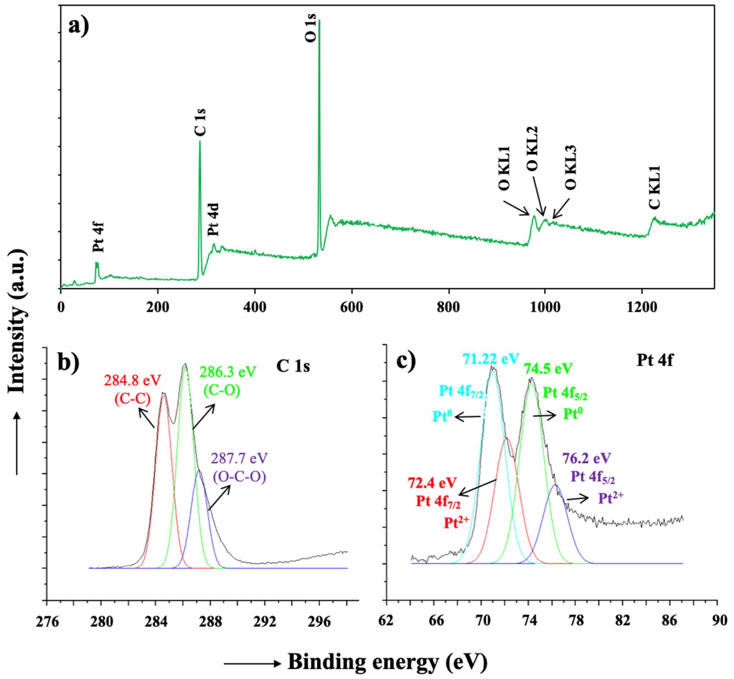

Figure 2. a) XPS survey spectrum of PtNPs@CF, b) high-resolution XPS spectra of C 1s, and c) Pt 4f.

The X-ray photoelectron survey spectrum indicated the presence of elements such as carbon, oxygen, and platinum in the PtNPs@CF, Figure 2a. The oxidation states and the bonding of the elements were further analyzed by the high-resolution X-ray photoelectron spectroscopy

(HRXPS) study. For example, relatively highly intense peaks of Pt 4f at 71.22 eV (Pt $4f_{7/2}$) and 74.5 eV(Pt $4f_{5/2}$) suggested the presence of metallic platinum (Pt^0) in the PtNPs, Figure 2c.[30,31] Two less intense peaks of Pt 4f at 72.4 eV (Pt $4f_{7/2}$) and 76.2 eV (Pt $4f_{5/2}$) indicated the presence of trace ionic platinum (Pt^{2+}) in the PtNPs.[24,25] Therefore, the HRXPS studies revealed that the PtNPs consisted of both metallic and ionic species of platinum. The Pt^0 XPS peaks could have originated from the metallic core of the PtNPts whereas, the Pt^{2+} peak originated from surface of the PtNPts. The ionic Pt^{2+} on the surface of the PtNPs can coordinate to the excess rhodizonate ions to become stabilized in water. This further indicates the binding ability of PtNPs with the cellulose fibers through the oxygen carrying functional groups of the cellulose.

Further, the PtNPs@CF was characterized by the Brunauer-Emmett-Teller (BET) specific surface area analysis, which was achieved by the nitrogen gas adsorption isotherms. The BET specific surface area of ~0.0816 m^2/g with pore volume of ~1.344 mm^3/g and a pore size of ~145.449 Å were measured for the PtNPs@CF.

4. Results and Discussion

Sodium borohydride is the most ubiquitously used reducing agent for the reduction of 4-nitrophenol and organic pollutants in water.[32,33,34,35] However, the excess sodium borohydride and its decomposition products remain in the reaction mixture. Therefore, the separation of the desired reaction products from the unexpected excess borohydride and its decomposition products becomes a difficult job. When used for the purpose of water treatment, the removal of the excess $NaBH_4$ and its decomposition products, also called as secondary pollutants, becomes a cumbersome job as well. Therefore, there is a need for the use of a clean, effective and environmentally benign reducing agent. In this aspect, although the use of hydrogen gas as a reducing agent is very common in organic synthesis, its use in the reduction of organic pollutants (viz. 4-NP and MO) in water is very scarce or not reported to the best of our knowledge. This study reports the use of hydrogen gas for the effective reduction of 4-NP in water, which could possibly be extended to the reduction of a wide variety of other organic and inorganic species such as organic dyes, polychlorinated organic compounds, hexavalent chromium, etc.

The synthesis of PtNPs was carried out by rapidly injecting the sodium rhodizonate solution into a boiling solution of chloroplatinic acid in water. The molar ratio (R) of the sodium rhodizonate to chloroplatinic acid was 3.88. Within 5 min period of heating, the reaction mixture transformed to an orange to brownish yellow color, which indicated the formation of the PtNPs. Since sodium rhodizonate was the only species used for the synthesis of the PtNPs, it could be considered that sodium rhodizonate performed as the reducing as well as stabilizing agent at the same time. The as-prepared PtNPs solution could be stored at room temperature in a laboratory drawer for more than 6 months period of time without observing the aggregation of the nanoparticles. As-synthesized PtNPs were supported on cellulose fibers obtained from Kimwipe paper. The Kimwipe paper was chosen as the source of cellulose fibers due to the macroporosity and chemical functionality, which could rapidly host or impregnate the PtNPs. Due to the polarized functional groups [(e.g. electron-rich oxygen atoms of polar hydroxyl (O-H) and ether groups and (O-C-O)] of the cellulose fibers, we assume that the PtNPs were strongly bound to cellulose fibers via the electrostatic and nonbonding interactions, Figure 1g. The Pt^{2+} ions at the surface of the PtNPs (revealed by the XPS study) can bind to the partially polarized oxygen atoms of the cellulose fibers through the ion-dipole interactions.[36]

The kinetics of the hydrogen gas mediated catalytic reduction of 4-NP was evaluated by the pseudo-first-order model with respect to 4-NP. The linear form of the pseudo-first-order reaction kinetic model could be expressed by the following equation.

$$-ln\frac{Ct}{Co} = kt \qquad (1)$$

where C_o and C_t represent the initial and time-dependent concentration of 4-NP, k (1/min) represents the pseudo-first-order rate constant.

The percent reduction of 4-NP was calculated using equation 2.

$$Reduction\ (\%) = \frac{C_0 - C_t}{C_0} = \frac{A_0 - A_t}{A_0} \times 100\% \qquad (2)$$

where A_0 and A_t represent the absorbance of 4-NP at concentrations C_0 and C_t, respectively.

4.1. Catalytic reduction of 4-NP using H_2 gas

Hydrogen gas assisted catalytic reduction 4-NP and the corresponding kinetics are shown in Figure 3. Time-dependent UV-Visible spectrum of 4-NP during its catalytic reduction on PtNPs@CF is shown in Figure 3a. A gradual decrease in the characteristic absorbance of 4-NP at 320 nm was observed. A new band originated at 300 nm, characteristic to 4-AP confirmed the reduction of 4-NP to 4-AP. On the other hand, the uncatalyzed reaction, where only cellulose fibers and hydrogen gas was used, did not show any lowering in the absorbance of 4-AP characteristic peaks after 16 min of reaction time, Figure 3b. About 1-2 percent of the 4-AP was found to be adsorbed on the Kimwipe paper. This indicates the ability of the PtNPs in the reduction of 4-AP in presence of hydrogen gas.

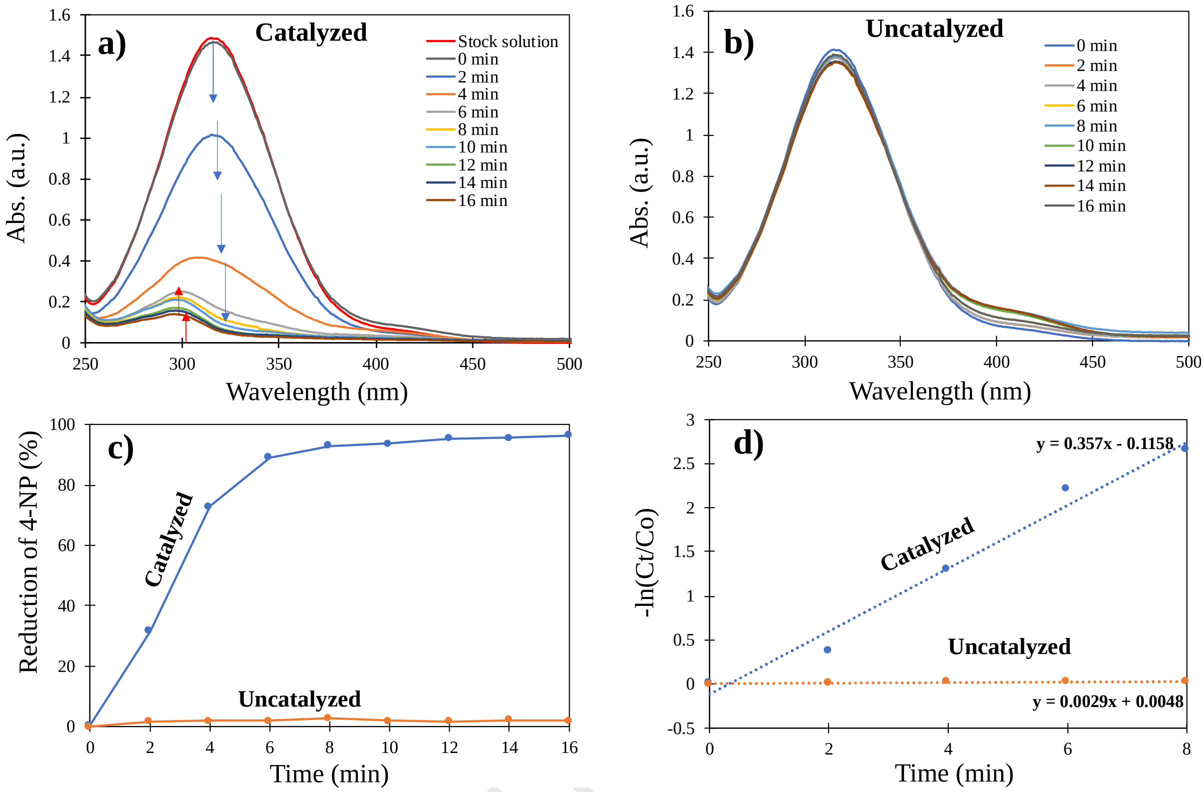

Figure 3. Time-dependent UV-visible spectrum of 4-NP during a) PtNPs@CF catalyzed and b) uncatalyzed reactions. Corresponding c) percent reduction and d) pseudo-first order kinetics of the 4-NP reduction.

The time-dependent percent reduction and the pseudo-first-order reaction kinetics for the catalytic reduction of 4-NP are shown in Figure 3c and 3d, respectively. It was observed that the PtNPs@CF reduced more the 93 percent of the 4NP in about 8 min of reaction time (calculated using Equation 2), Figure 3c. On the other hand, the uncatalyzed reaction did not reduce 4-NP at all even after 16 min of reaction time. About 1-2 percent of 4-NP removal was obtained for the uncatalyzed reaction, which was mainly because of adsorption of 4-NP on the CF, Figure 3c. The apparent rate constant (k_{app}) for the PtNPs@CF catalyzed reaction was calculated from the slope of the -ln(C_t/C_0) versus time (t) curve, Equation 1. The k_{app} for the PtNPs@CF catalyzed and uncatalyzed reactions were 3.6×10^{-1} min^{-1} and 2.9×10^{-3} min^{-1}, respectively. From the k_{app}

values it was found that the PtNPs@CF catalyzed reaction was about 125-fold faster than the uncatalyzed reaction.

4.2. Catalytic reduction of MO using H_2 gas

The UV-Visible spectrum of MO during the catalytic reduction is shown in Figure 4a. It was observed that the characteristic absorbance of MO at 464 and 275 nm diminished gradually while a new peak originated at 245 nm. Due to the conjugation throughout the structure and the azo (-N=N-) bond MO gives characteristic peaks at 464 and 275 nm, respectively. The disappearance of these two characteristic peaks indicate the loss of conjugation due to the break of the azo (-N=N-) bond. The rise of a new peak at 245 nm is characteristic to the reduction products such as hydrazine derivatives of MO, 4-aminobenzenesulfonate, and 4-N,N-dimenthylaminobenzene.[37]

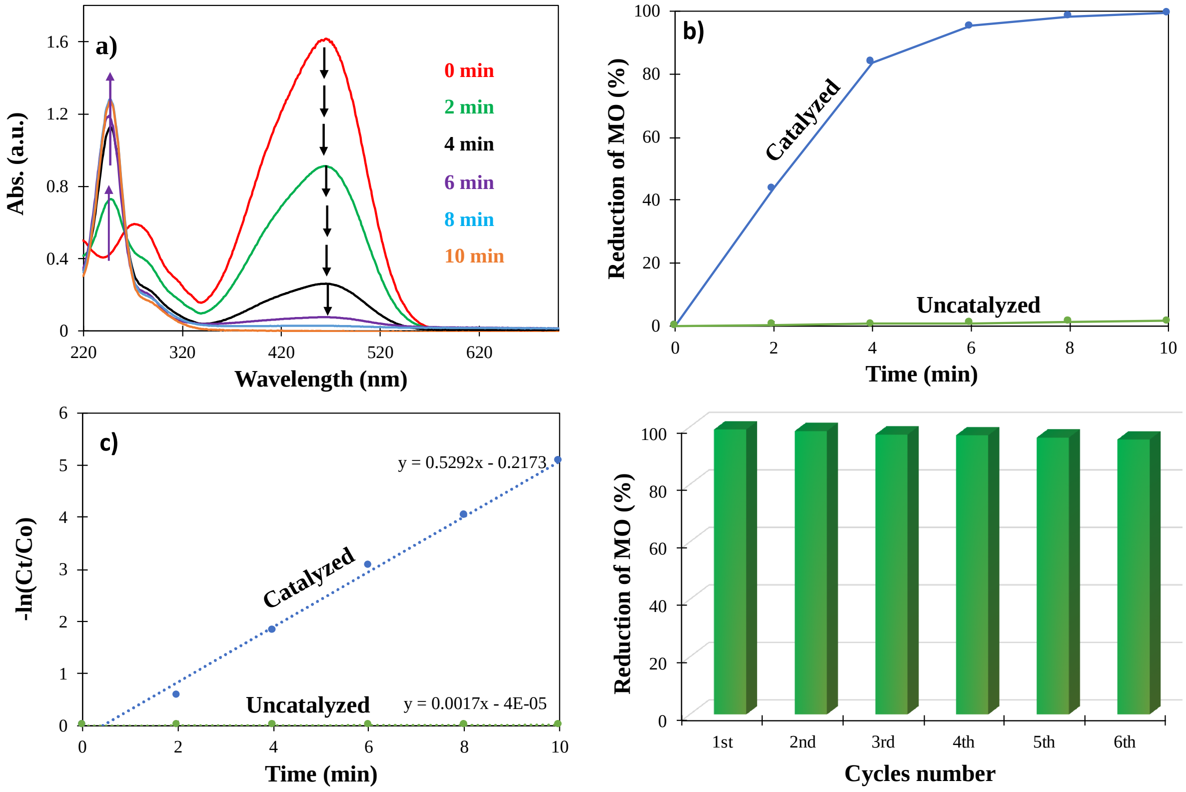

Figure 4. a) Time-dependent UV-visible spectrum of MO solution during the PtNPs@CF catalyzed reaction, b) time-dependent percent reduction of MO, c) corresponding pseudo-first-order kinetics of MO reduction, and cyclic stability of PtNPs@CF for the reduction of MO.

The kinetics of the reaction showed that about 99 % MO was reduced after 10 min of reaction, Figure 4b. The reaction where no catalyst was used showed about 1.6 % decolorization of MO due to adsorption of the cellulose fibers, Figure 4b. The reaction followed the pseudo-first-order kinetics and k_{app} was calculated to be 5.3×10^{-1}min^{-1}, whereas; the k_{app} of the uncatalyzed reaction was calculated to be 1.710^{-1} min^{-1}.

The cyclic stability of the PtNPs@CF was studied for six cycles and it was found that the catalyst was fairly stable throughout the cycles of use, Figure 4d. Negligible decrease in the catalytic activity was observed, which indicated robustness of the PtNPs@CF for multiple cylces of use.

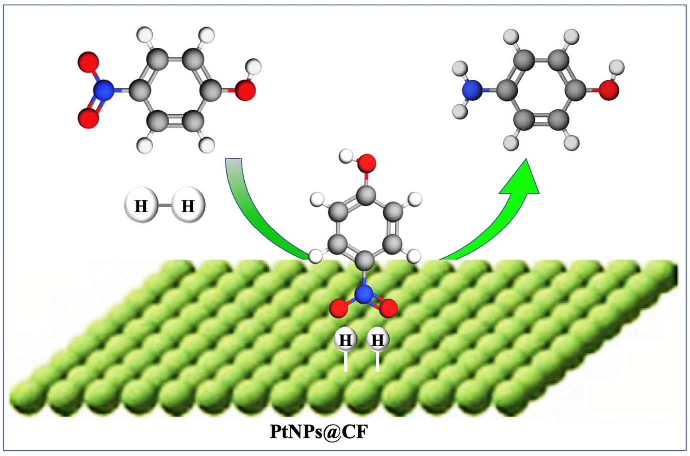

Scheme 1. H_2 gas-assisted catalytic reduction of 4-NP on PtNPs@CF.

A well-accepted mechanism for the hydrogen gas-assisted reduction of 4-NP on PtNPs@CF can be briefly be described as of Scheme 1. The H_2 gas adsorbs to the PtNPs surface with partial or complete cleavage of the H-H bond, also known as the chemisorption of the H_2 gas. The pi bond of the nitro group of the 4-NP complexes with the PtNPs. Afterward, the chemisorbed H atoms are transferred sequentially to the pi bond of the nitro group forming 4-AP causing the reduction of the 4-NP. The reaction product viz 4-AP is then released from the PtNPs.

4.3. Comparison with Literature

The catalytic performance of PtNPs@CF for the reduction of 4-NP and MO was further compared with various other noble and transition metal nanoparticles catalysts, Table 1. However, most of the studies available in literature reported the use of $NaBH_4$ as reducing agent. Therefore, following table compares the catalytic activity of different catalysts in reducing 4-NP and MO by H_2 gas and $NaBH_4$.

Table 1. Catalytic performance of PtNPs@CF compared with other noble and transition metal catalysts.

Catalysts	Substrate	Reducing agent	Rate constant (min^{-1})	Reference
PtNPs@CF	MO	H_2	5.3×10^{-1}	This work
PtNPs@CF	4-NP	H_2	3.6×10^{-1}	This work
Au/SNTs	4-NP	$NaBH_4$	1.8×10^{-2}	[38]
$AuNPs@TiO_2$	4-NP	$NaBH_4$	6.3×10^{-1}	[39]
AuNPs@MWCNT	4-NP	$NaBH_4$	6.6×10^{-3}	[40]
Dendrimer-PdNC	4NP	$NaBH_4$	1.1×10^{-1}	[41]
PtNPs@polymer brush	4-NP	$NaBH_4$	5.7×10^{-1}	[42]
PET2-APTES-Ag/Cu	4-NP	$NaBH_4$	1.77×10^{-1}	[22]
PC-CuO-DEA	4-NP	$NaBH_4$	3.69×10^{-1}	[32]
PET-Fe PET-APTES-Fe PET-PAMAM-Fe PET-SH-Fe	4-NP	$NaBH_4$	2.52×10^{-2} 4.58×10^{-2} 2.44×10^{-2} 6.60×10^{-2}	[35]
AuNPs@CF	MO	$NaBH_4$	2.75×10^{-1}	[43]
Ni-sponge	MO	$NaBH_4$	2.28×10^{-1}	[44]
Cu-NRds	MO	$NaBH_4$	2.16×10^{-1}	[45]
Ag nanostructures	MO	$NaBH_4$	3.35×10^{-2}	[46]

AuNPs	MO	$NaBH_4$	1.02×10^{-1}	[47]

The comparison table demonstrates that the H_2 gas assisted catalytic reduction of 4-NP and MO on PtNPs@CF is faster than the catalytic performance of some noble metal nanoparticles-based catalysts. The PtNPs@CF also showed slower activity compared to some other catalytic systems, which could be due to the use of a large excess of $NaBH_4$ in those systems. However, due to environmental benignity, cleanliness, and facility of the process, H_2 gas assisted catalytic reduction can be considered as an alternative reducing agent for the reduction of environmental pollutants in water. Additionally, as the reducing agent H_2 gas can be utilized for the catalytic reduction of a wide spectrum of organic and inorganic compounds.

5. Conclusions and summary

We have presented the catalytic reduction of hazardous organic pollutants (4-nitrophenol and methyl orange) on platinum nanoparticles immobilized on cellulose fibers. Platinum nanoparticles of about 2 nm in size were synthesized, which demonstrated high catalytic activty in the reduction of organic pollutants in presence of hydrogen gas as the reducing agent. Hydrogen gas was used as the clean and environmentally benign reducing agent alternative to $NaBH_4$. Excellent catalytic activity was obtained under the ambient experimental conditions and the reaction kinetics followed the pseudo-first-order model. Since hydrogen gas does not generate any secondary pollutants, it could potentially be utilized as a clean, efficient, and environmentally friendly reducing agent for the reduction of organic pollutants such as halogenated organic compounds, pharmaceuticals, antibiotics, and so on.

Acknowledgements

Financial support from the National Science Foundation (NSF) grants ERC Nanotechnology-Enabled Water Treatment Center 1449500, CHE-0748913, DMR PREM-1205302, and USDA 2014-38422-22078 are gratefully acknowledged.

Author Information

Corresponding Author:

Md Tariqul Islam, Email: islam_m@utpb.edu / tariqul.lab@gmail.com

Juan C. Noveron, Email: jcnoveron@utep.edu

Notes

The authors declare no conflicting financial interest.

Graphical abstract

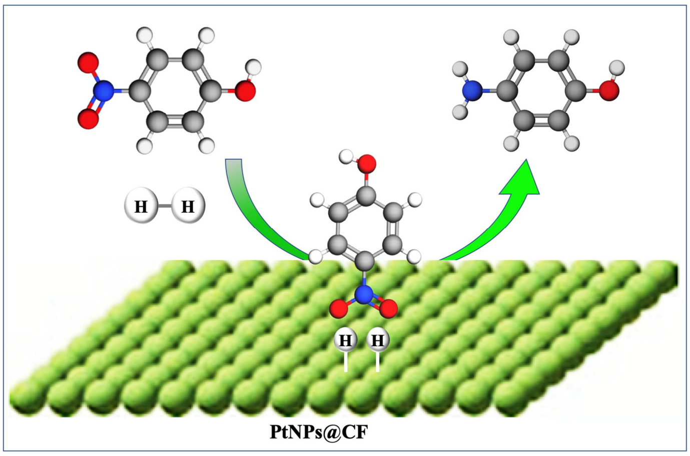

Hydrogen gas as the clean and alternative reducing agent for the catalytic reduction of 4-nitrophenol and methyl orange on platinum nanoparticles supported on cellulose fibers.

References:

---

[1] Lin, X. Q., Deng, H. H., Wu, G. W., Peng, H. P., Liu, A. L., Lin, X. H., ... & Chen, W. (2015). Platinum nanoparticles/graphene-oxide hybrid with excellent peroxidase-like activity and its application for cysteine detection. Analyst, 140(15), 5251-5256.

---

[2] Qin, Y., Chao, L., Yuan, J., Liu, Y., Chu, F., Kong, Y., ... & Liu, M. (2016). Ultrafine Pt nanoparticle-decorated robust 3D N-doped porous graphene as an enhanced electrocatalyst for methanol oxidation. Chemical Communications, 52(2), 382-385.

[3] Eustis, S., & El-Sayed, M. A. (2006). Why gold nanoparticles are more precious than pretty gold: noble metal surface plasmon resonance and its enhancement of the radiative and nonradiative properties of nanocrystals of different shapes. Chemical society reviews, 35(3), 209-217.

[4] Lopez, N., Janssens, T. V. W., Clausen, B. S., Xu, Y., Mavrikakis, M., Bligaard, T., & Nørskov, J. K. (2004). On the origin of the catalytic activity of gold nanoparticles for low-temperature CO oxidation. *Journal of Catalysis*, *223*(1), 232-235.

[5] Sánchez-Sánchez, C. M., Solla-Gullón, J., Vidal-Iglesias, F. J., Aldaz, A., Montiel, V., & Herrero, E. (2010). Imaging structure sensitive catalysis on different shape-controlled platinum nanoparticles. Journal of the American Chemical Society, 132(16), 5622-5624.

[6] Wand, P., Kratzer, E., Heiz, U., Cokoja, M., & Tschurl, M. (2017). High stability of thiol-protected colloidal platinum nanoparticles with reduced ligand coverages in the hydrogenation of 3-hexyne. Catalysis Communications, 100, 85-88.

[7] Kong, F. D., Yin, G. P., Du, C. Y., Zhang, S., Qu, Y. T., Du, L., ... & Ling, A. X. (2015). 3D-niobium oxide supported platinum as an effective and durable oxygen reduction catalyst. Catalysis Communications, 68, 67-72.

[8] Uson, L., Hueso, J. L., Sebastian, V., Arenal, R., Florea, I., Irusta, S., ... & Santamaria, J. (2017). In-situ preparation of ultra-small Pt nanoparticles within rod-shaped mesoporous silica particles: 3-D tomography and catalytic oxidation of n-hexane. Catalysis Communications, 100, 93-97.

---

[9] Bell, A. T. (2003). The impact of nanoscience on heterogeneous catalysis. Science, 299(5613), 1688-1691.

[10] Mandal, S., Roy, D., Chaudhari, R. V., & Sastry, M. (2004). Pt and Pd nanoparticles immobilized on amine-functionalized zeolite: excellent catalysts for hydrogenation and heck reactions. Chemistry of materials, 16(19), 3714-3724.

[11] Lv, Z. S., Zhu, X. Y., Meng, H. B., Feng, J. J., & Wang, A. J. (2019). One-pot synthesis of highly branched Pt@Ag core-shell nanoparticles as a recyclable catalyst with dramatically boosting the catalytic performance for 4-nitrophenol reduction. *Journal of colloid and interface science*, *538*, 349-356.

[12] Zhu, X. Y., Lv, Z. S., Feng, J. J., Yuan, P. X., Zhang, L., Chen, J. R., & Wang, A. J. (2018). Controlled fabrication of well-dispersed AgPd nanoclusters supported on reduced graphene oxide with highly enhanced catalytic properties towards 4-nitrophenol reduction. *Journal of colloid and interface science*, *516*, 355-363.

[13] Zhang, X. F., Zhu, X. Y., Feng, J. J., & Wang, A. J. (2018). Solvothermal synthesis of N-doped graphene supported PtCo nanodendrites with highly catalytic activity for 4-nitrophenol reduction. *Applied Surface Science*, *428*, 798-808.

[14] Xia, Y., Gao, Z., Liao, X., Yan, S., Han, J., Wang, X., ... & Zhai, W. (2018). One-step green synthesis of silver nanobelts assisted by sodium carboxymethylcellulose for catalytic reduction of 4-nitrophenol. CrystEngComm, 20(15), 2135-2143.

[15] Islam, M. T., Padilla, J. E., Dominguez, N., Alvarado, D. C., Alam, M. S., Cooke, P., ... & Noveron, J. C. (2016). Green synthesis of gold nanoparticles reduced and stabilized by squaric acid and supported on cellulose fibers for the catalytic reduction of 4-nitrophenol in water. RSC Advances, 6(94), 91185-91191.

---

[16] Lewis, R.J. Sr.; Hawley's Condensed Chemical Dictionary 15th Edition. John Wiley & Sons, Inc. New York, NY 2007., p.62

[17] Ashford, Robert D. Ashford's dictionary of industrial chemicals: properties, production, uses. Wavelength, 1994.

[18] O'Neil, M. J., Smith, A., Heckelman, P. E., & Budavari, S. (2001). The Merck Index-An Encyclopedia of Chemicals, Drugs, and Biologicals. Whitehouse Station, NJ: Merck and Co. Inc, 767, 4342.

[19] Mitchel CS et al; Kirk-Othmer Encyclopedia of Chemical Technology. (2001). New York, NY: John Wiley & Sons; Aminophenols. Online Posting Date: Jun 20, 2003.

[20] Yan, Z., Fu, L., Zuo, X., & Yang, H. (2018). Green assembly of stable and uniform silver nanoparticles on 2D silica nanosheets for catalytic reduction of 4-nitrophenol. Applied Catalysis B: Environmental, 226, 23-30.

[21] Li, J., Liu, C. Y., & Liu, Y. (2012). Au/graphene hydrogel: synthesis, characterization and its use for catalytic reduction of 4-nitrophenol. Journal of Materials Chemistry, 22(17), 8426-8430.

[22] Nabil, B., Morshed, M. N., Nemeshwaree, B., Christine, C., Julien, V., Olivier, T., & Abdelkrim, A. (2019). Development of new multifunctional filter based nonwovens for organics pollutants reduction and detoxification: High catalytic and antibacterial activities. Chemical Engineering Journal, 356, 702-716.

[23] Lowry, G. V.; Reinhard, M. Hydrodehalogenation of 1-to 3-carbon halogenated organic compounds in water using a palladium catalyst and hydrogen gas. Environ. Sci. Technol. **1999**, 33, 1905-1910.

[24] Niu, H. J., Chen, H. Y., Wen, G. L., Feng, J. J., Zhang, Q. L., & Wang, A. J. (2019). One-pot solvothermal synthesis of three-dimensional hollow PtCu alloyed dodecahedron nanoframes with

excellent electrocatalytic performances for hydrogen evolution and oxygen reduction. *Journal of colloid and interface science*, *539*, 525-532.

[25] Chen, H. Y., Jin, M. X., Zhang, L., Wang, A. J., Yuan, J., Zhang, Q. L., & Feng, J. J. (2019). One-pot aqueous synthesis of two-dimensional porous bimetallic PtPd alloyed nanosheets as highly active and durable electrocatalyst for boosting oxygen reduction and hydrogen evolution. *Journal of colloid and interface science, 543*, 1-8.

[26] Islam, M. T., Rosales, J., Ricardo, S. A., Ghadimi, S., & Noveron, J. Rapid Synthesis of Ultrasmall Platinum Nanoparticles Supported on Macroporous Cellulose Fibers for Catalysis. *Nanoscale Adv*., 2019, **1**, 2953-2964.

[27] Watanabe, K.; Tabuchi, M.; Morinaga Y.; Yoshinaga, F., Structural Features and Properties of Bacterial Cellulose Produced in Agitated Culture. Cellulose, **1998**, 5, 187–200.

[28] Lee, C.M.; Gu, J.; Kafle, K.; Catchmark J.; Kim, S.H., Cellulose produced by Gluconacetobacter xylinus strains ATCC 53524 and ATCC 23768: Pellicle formation, post-synthesis aggregation and fiber density. Carbohydr. Polym., **2015**, 133, 270–276.

[29] Islam, M. T., Saenz-Arana, R., Wang, H., Bernal, R., & Noveron, J. C. (2018). Green synthesis of gold, silver, platinum, and palladium nanoparticles reduced and stabilized by sodium rhodizonate and their catalytic reduction of 4-nitrophenol and methyl orange. New Journal of Chemistry, 42(8), 6472-6478.

[30] Wang, T., Yang, R., Ouyang, S., Shi, H., & Wang, S. (2015). Light-induced synthesis of clean-surface PdPt@ Pt core–shell nanoparticles with excellent electrocatalytic activity. RSC Advances, 5(60), 48992-48996.

---

[31] Şen, F., & Gökağaç, G. (2007). Different sized platinum nanoparticles supported on carbon: an XPS study on these methanol oxidation catalysts. The Journal of Physical Chemistry C, 111(15), 5715-5720.

[32] Nabil, B., Ahmida, E. A., Christine, C., Julien, V., & Abdelkrim, A. (2019). Inorganic-organic-fabrics based polyester/cotton for catalytic reduction of 4-nitrophenol. Journal of Molecular Structure, 1180, 523-531.

[33] Sahiner, N., Sagbas, S., & Aktas, N. (2015). Very fast catalytic reduction of 4-nitrophenol, methylene blue and eosin Y in natural waters using green chemistry: p (tannic acid)–Cu ionic liquid composites. RSC Advances, 5(24), 18183-18195.

[34] Ajmal, M., Siddiq, M., Al-Lohedan, H., & Sahiner, N. (2014). Highly versatile p (MAc)–M (M: Cu, Co, Ni) microgel composite catalyst for individual and simultaneous catalytic reduction of nitro compounds and dyes. RSC Advances, 4(103), 59562-59570.

[35] Morshed, M. N., Bouazizi, N., Behary, N., Vieillard, J., Thoumire, O., Nierstrasz, V., & Azzouz, A. (2019). Iron-loaded amine/thiol functionalized polyester fibers with high catalytic activities: a comparative study. Dalton Transactions.

[36] He, J., Kunitake, T., & Nakao, A. (2003). Facile in situ synthesis of noble metal nanoparticles in porous cellulose fibers. *Chemistry of Materials*, *15*(23), 4401-4406.

[37] Johnstone, R. A. W.; & Wilby, A. H., Heterogeneous catalytic transfer hydrogenation and its relation to other methods for reduction of organic compounds. Chem. Rev., **1985**, 85, 129–170.

[38] Jan, J. S., Chuang, T. H., Chen, P. J., & Teng, H. (2011). Layer-by-layer polypeptide macromolecular assemblies-mediated synthesis of mesoporous silica and gold nanoparticle/mesoporous silica tubular nanostructures. Langmuir, 27(6), 2834-2843.

---

[39] Islam, M. T., Jing, H., Yang, T., Zubia, E., Goos, A. G., Bernal, R. A., ... & Noveron, J. C. (2018). Fullerene stabilized gold nanoparticles supported on titanium dioxide for enhanced photocatalytic degradation of methyl orange and catalytic reduction of 4-nitrophenol. Journal of environmental chemical engineering, 6(4), 3827-3836.

[40] Abdel-Fattah, T. M., & Wixtrom, A. (2014). Catalytic reduction of 4-nitrophenol using gold nanoparticles supported on carbon nanotubes. ECS Journal of Solid State Science and Technology, 3(4), M18-M20.

[41] Esumi, K., Isono, R., & Yoshimura, T. (2004). Preparation of PAMAM− and PPI− metal (silver, platinum, and palladium) nanocomposites and their catalytic activities for reduction of 4-nitrophenol. Langmuir, 20(1), 237-243.

[42] Mei, Y., Sharma, G., Lu, Y., Ballauff, M., Drechsler, M., Irrgang, T., & Kempe, R. (2005). High catalytic activity of platinum nanoparticles immobilized on spherical polyelectrolyte brushes. Langmuir, 21(26), 12229-12234.

[43] Islam, M. T., Dominguez, N., Ahsan, M. A., Dominguez-Cisneros, H., Zuniga, P., Alvarez, P. J., & Noveron, J. C. (2017). Sodium rhodizonate induced formation of gold nanoparticles supported on cellulose fibers for catalytic reduction of 4-nitrophenol and organic dyes. Journal of environmental chemical engineering, 5(5), 4185-4193.

[44] Islam, M. T., Rosales, J., Ricardo, S. A., Arrieta, R., Kim, H., Sultana, K. A., ... & Noveron, J. (2019). Synthesis of high-surface area transition metal sponges and their catalytic properties. New Journal of Chemistry.

[45] Soomro, R. A., & Nafady, A. (2015). Catalytic reductive degradation of methyl orange using air resilient copper nanostructures. Journal of Nanomaterials, 16(1), 120.

---

[46] Sakir, M., & Onses, M. S. (2019). Solid substrates decorated with Ag nanostructures for the catalytic degradation of methyl orange. Results in Physics, 12, 1133-1141.

[47] Umamaheswari, C., Lakshmanan, A., & Nagarajan, N. S. (2018). Green synthesis, characterization and catalytic degradation studies of gold nanoparticles against congo red and methyl orange. Journal of Photochemistry and Photobiology B: Biology, 178, 33-39.

Highlights:

- Synthesis of cellulose fibers supported platinum nanoparitcles.
- Hydrogen gas-assisted fast reduction of 4-nitrophenol & methyl orange.
- Excellent catalytic activity and stability of the nanocomposite.
- Hydrogen gas is a clean reducing agent alternative to $NaBH_4$.

Conflict of interest form

for

Borohydride-free catalytic reduction of organic pollutants by platinum nanoparticles supported on cellulose fibers

Md. Tariqul Islam,[abc*] Kazi Afroza Sultana,[d] Juan C. Noveron [ab*]

[a] Department of Chemistry and Biochemistry, University of Texas at El Paso, 500 West University Avenue, El Paso, TX 79968, USA

[b] NSF Nanosystems Engineering Research Center for Nanotechnology Enabled Water Treatment (NEWT)

[c] Department of Chemistry, University of Texas of the Permian Basin, 4901 E University Blvd, Odessa, TX 79762

[d] Department of Environmental Science and Engineering, University of Texas at El Paso, 500 West University Avenue, El Paso, TX 79968, USA

Authors declare no conflicting interest of any type.

Sincerely,
Md Tariqul Islam, Ph.D.
Senior Lecturer of Chemistry
University of Texas Permian Basin
4901 E University Blvd, Odessa, TX 79762

Fax: 432-552-3230 Tel: 765-749-2505
E-mail: islam_m@utpb.edu